Electronic supplementary information

Pyrene and imidazole functionalized luminescent bimetallic Ru(II) terpyridine complexes as efficient optical chemosensors for cyanide in aqueous, organic and solid media

Srikanta Karmakar, Dinesh Maity, Sourav Mardanya and Sujoy Baitalik*

Table of Contents:

Experimental Section

Physical Measurements. NMR spectra of the complexes were recorded on a Bruker 300 spectrometer in DMSO–d_6. UV-vis absorption spectra were recorded using a Shimadzu UV 1800 spectrometer at room temperature. Steady state luminescence spectra were obtained either by Perkin–Elmer LS55 spectrofluorometer. Luminescence quantum yields were determined using literature method taking $[Ru(bpy)_3]^{2+}$ for metal complexes and quinine sulphate for ligand as the

standard. Luminescence lifetime measurements were carried out by using time–correlated single photon counting set up from Horiba Jobin-Yvon. The luminescence decay data were collected on a Hamamatsu MCP photomultiplier (R3809) and were analyzed by using IBH DAS6 software.

The sensing studies of the complexes (**1-3**) with different anions were carried out in DMSO (~10.0 μM) as well as in DMSO-water medium (1**:**100) (~10.0 μM). Tetrabutylammonium (TBA) salts of different anions were used for titration experiments. On the other hand, for a typical absorption and emission titration experiment, 1μL aliquot of a given anion (10 mM) was added successively to a 2.5 mL solution of the metal complexes (~10.0 μM). The binding/equilibrium constant towards anion were evaluated from the absorbance data using equation (1).

$$A_{obs} = (A_0 + A_\infty K[G]_T)/(1+ K[G]_T) \quad (1)$$

where A_{obs} is the observed absorbance, A_0 is the absorbance of the free receptor, A_∞ is the maximum absorbance induced by the presence of a given anionic guest, $[G]_T$ is the total concentration of the guest, and K is the binding/equilibrium constant of the host–guest entity. Binding constants were performed in duplicate, and the average value is reported.

Experimental uncertainties were as follows: absorption maxima, ±2 nm; molar absorption coefficients, 10%; emission maxima, ±5 nm; excited–state lifetimes, 10%; luminescence quantum yields, 20%.

Theoretical Calculation Methods. Quantum chemical calculations were performed with the Gaussian 09 program.[S1] The geometries of the ground-state (S_0) were optimized by means of density functional theory using the exchange-correlation functional B3LYP.[S2,S3] The 6-31G(d) basis set was employed for the C, H and N while SDD basis set was used for Ru atom. The singlet excited state geometries corresponding to the vertical excitations were optimized using the time-dependent DFT (TDDFT) scheme to compute the UV-vis transitions of the compounds, starting with the ground state geometries optimized in solution phase.[S4-S7] The effects of the interaction with solvent DMSO (ε = 46.826) on the geometries and excitation energies were taken into account by the integral equation formalism of the conductor-like polarizable continuum model (CPCM).[S8] UKS calculations were also performed directly on the triplet state of the complexes to calculate singlet-triplet energy gap. Orbital analysis was completed with Gauss View[S9] and Gauss sum 2.2[S10].

Table S1 Selected calculated bond distances (Å) for complexes **1-3** and **1a-3a** in the ground state in DMSO.

	sol					
	1	**2**	**3**	**1a**	**2a**	**3a**
Ru1-N6	2.109	2.111	2.122	2.109	2.111	2.117
Ru1-N2	2.007	2.006	2.000	2.009	2.009	1.985
Ru1-N4	2.109	2.111	2.120	2.109	2.110	2.118
Ru1-N5	2.010	2.008	2.042	2.008	2.006	2.059
Ru1-N1	2.111	2.111	2.109	2.111	2.112	2.098
Ru1-N3	2.111	2.111	2.108	2.112	2.110	2.097
Ru2-N'4	2.109	2.111	2.122	2.109	2.110	2.118
Ru2- N'5	2.010	2.006	2.000	2.008	2.006	2.059
Ru2- N'6	2.110	2.111	2.108	2.109	2.111	2.117
Ru2- N'1	2.111	2.111	2.042	2.111	2.112	2.098
Ru2- N'2	2.007	2.111	2.109	2.009	2.009	1.985
Ru2- N'3	2.111	2.008	2.120	2.112	2.110	2.097

Table S2 Selected calculated bond angles (deg) for**1-3** and **1a-3a** in the ground optimized states in DMSO.

	1	**2**	**3**	**1a**	**2a**	**3a**
N6Ru1N2	101.9	102.1	102.3	101.8	101.9	102.3
N6Ru1N4	157.0	156.7	154.9	157.1	156.8	154.5
N6Ru1N5	78.5	78.3	77.4	78.5	78.3	77.3
N6Ru1N1	92.2	92.2	92.7	92.2	92.1	92.5
N2Ru1N3	78.4	78.4	78.5	78.2	78.3	78.8
N2Ru1N4	100.9	101.0	102.3	101.0	101.2	103.0
N2Ru1N1	78.3	78.4	78.5	78.3	78.2	78.7
N3Ru1N6	92.1	92.2	92.1	92.3	92.4	92.5
N4Ru1N5	78.5	78.3	77.4	78.5	78.4	77.2
N4Ru1N1	92.2	92.3	92.2	92.2	92.3	92.3
N4Ru1N3	92.4	92.4	92.4	92.3	92.3	92.4
N5Ru1N1	101.7	101.7	101.5	101.8	102.0	101.4
N5Ru1N3	101.4	101.4	101.3	101.5	101.3	101.0
N1Ru1N3	156.8	156.8	157.0	156.6	156.6	157.5
N'2Ru2N'3	78.4	78.4	78.5	78.2	78.3	78.8
N'2Ru2 N'1	78.3	78.4	78.5	78.3	78.2	78.7
N'2Ru2 N'4	101.3	101.0	102.6	100.9	101.2	103.0
N'2Ru2 N'6	101.5	101.0	102.3	101.8	101.9	102.3
N'3Ru2 N'1	156.8	156.8	157.0	156.6	156.6	157.5
N'3Ru2 N'4	92.5	92.2	92.4	92.3	92.3	92.4
N'3Ru2 N'5	101.7	101.4	101.3	101.5	101.3	101.0
N'3Ru2 N'6	92.1	92.2	92.4	92.3	92.4	92.5
N'1Ru2 N'4	92.2	92.2	92.1	92.2	92.3	92.3
N'1Ru2 N'5	101.4	101.7	101.3	101.8	102.0	101.4
N'1Ru2 N'6	92.1	92.3	92.7	92.2	92.1	92.5
N'4Ru2 N'5	78.5	78.3	77.4	78.5	78.4	77.2
N'4Ru2 N'6	157.0	156.7	154.9	157.1	156.8	154.5
N'5Ru2 N'6	78.5	78.3	77.4	78.5	78.3	77.3

Table S3 Selected calculated bond distances (Å) for complexes **1a** and **3a** in the UKS optimized state in DMSO.

	UKS optimized state	
	1a	**3a**
Ru1-N6	2.107	2.121
Ru1-N2	2.012	1.992
Ru1-N4	2.107	2.122
Ru1-N5	2.003	2.053
Ru1-N1	2.110	2.099
Ru1-N3	2.110	2.098
Ru2-N'2	2.012	1.992
Ru2- N'3	2.110	2.098
Ru2- N'1	2.110	2.099
Ru2- N'4	2.107	2.122
Ru2- N'5	2.003	2.053
Ru2- N'6	2.107	2.121

Table S4 Selected calculated bond angles (deg) for **1a-3a** in the UKS optimized states in DMSO.

UKS optimized state		
	1a	**3a**
N6Ru1N2	101.6	102.2
N6Ru1N4	157.3	154.8
N6Ru1N5	78.6	77.4
N6Ru1N1	92.1	92.4
N6Ru1N3	92.4	92.6
N2Ru1N4	100.9	102.9
N2Ru1N3	78.1	78.6
N4Ru1N5	78.7	77.3
N4Ru1N1	92.2	92.4
N4Ru1N3	92.3	92.4
N5Ru1N1	102.0	101.6
N5Ru1N3	101.6	101.1
N1Ru1N3	156.3	157.1
N5Ru1N2	179.6	179.5
N'2Ru2N´3	78.1	78.6
N'2Ru2 N´1	78.1	78.5
N'2Ru2 N´4	100.9	102.9
N'2Ru2 N´5	179.6	179.5
N'2Ru2 N´6	101.6	102.2
N´5Ru2 N´1	102.0	101.6
N'3Ru2 N'4	92.3	92.4
N'3Ru2 N´5	101.6	101.1
N'3Ru2 N´6	92.4	92.6
N'1Ru2 N´4	92.2	92.4
N'1Ru2N´5	102.0	101.6
N'1Ru2N´6	92.1	92.4
N'4Ru2 N´5	78.7	77.3
N'4Ru2 N´6	157.3	154.8
N'5Ru2N´6	78.6	77.4
N'1Ru2N´3	156.3	157.1

Table S5 Selected MOs along with their energies and compositions for **1a** and **3a** in UKS optimized state.

MO	Energy, eV	(%) Composition				
	Sol^n	sol^n				
1a		tpycap	ph	ligtpy	Pyrene imida	Ru
L+3	-2.38	58.37	0.26	38.12	0.00	3.23
L+2	-2.47	40.07	0.37	59.48	0.00	0.05
L+1	-2.59	89.92	0.02	1.90	0.00	8.14
L	-2.68	1.81	6.00	82.39	2.03	7.74
H	-3.04	1.62	6.56	82.52	2.11	7.16
H-1	-4.95	0.26	14.55	2.98	80.03	2.16
H-2	-5.29	1.07	24.80	6.34	58.37	9.40
H-3	-5.55	0.02	0.02	0.03	98.01	1.09
3a		py26	ph	ligtpy	pyrenei mida	Ru
L+3	-1.46	93.35	0.00	0.99	0.00	5.65
L+2	-1.58	0.38	0.76	95.90	0.01	2.94
L+1	-2.08	0.15	0.69	96.93	0.00	2.22
L	-2.25	1.93	6.77	77.79	2.27	11.21
H	-2.65	1.70	7.73	78.46	2.47	9.63
H-1	-4.40	33.31	0.01	11.23	0.00	55.42
H-2	-4.75	1.60	14.21	5.51	64.41	14.25
H-3	-4.79	2.52	0.00	7.72	80.10	10.73

Table S6 Phosphorescence emission of the complexes **1a** and **3a** in DMSO according to UKS-calculations and associated experimental values.

	Energy for singlet state ($E1$/Hartree)	Energy for triplet state ($E2$/Hartree)	Emission energy $\Delta E=(E2- E1)$/ (eV)	λemission (theo)/nm	λemission (expt)/nm
1a	-4529.3021	-4529.2585	1.18	1045	----
3a	-5053.7670	-5053.7090	1.57	785	820

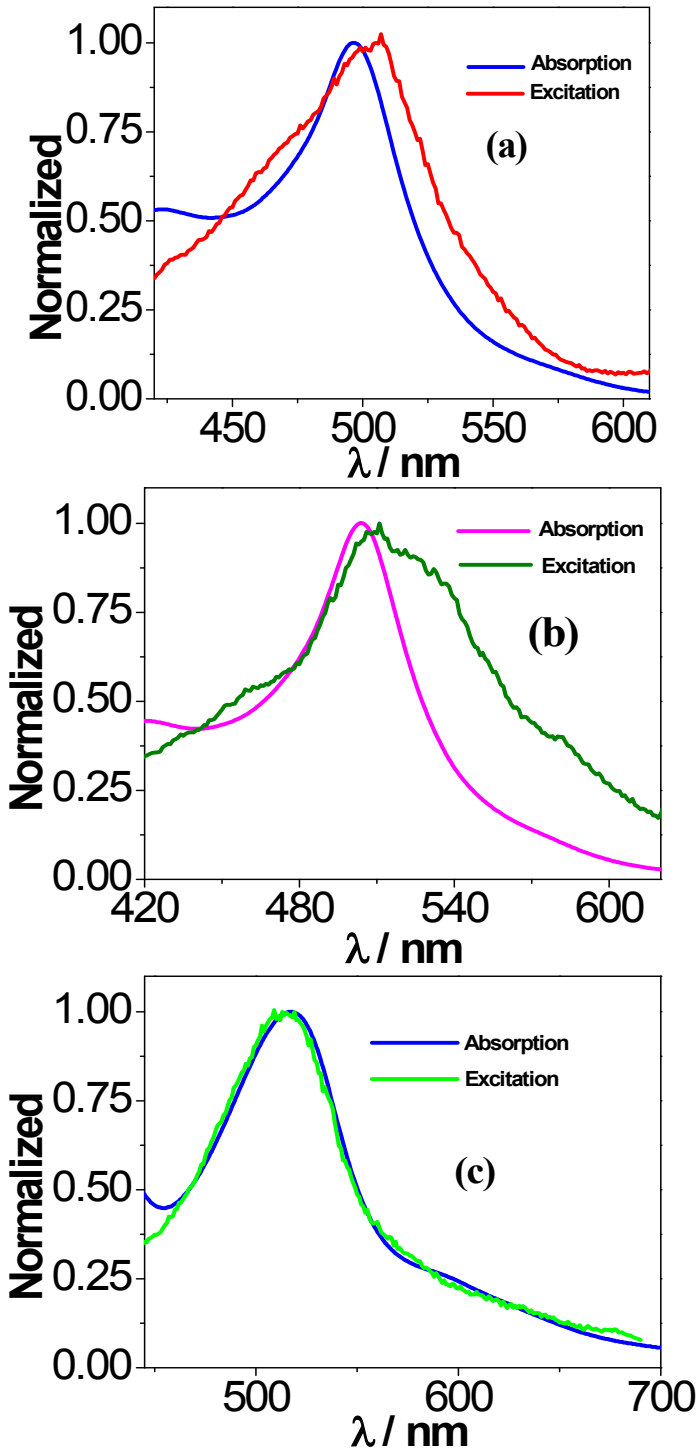

Fig. S1 Overlay of the normalized luminescence excitation and absorption spectrum of **1** (a), **2** (b), and **3** (c) in DMSO. The monitoring emission wavelength is 664 nm for **1**, 670 nm for **2**, and 703 nm for **3**.

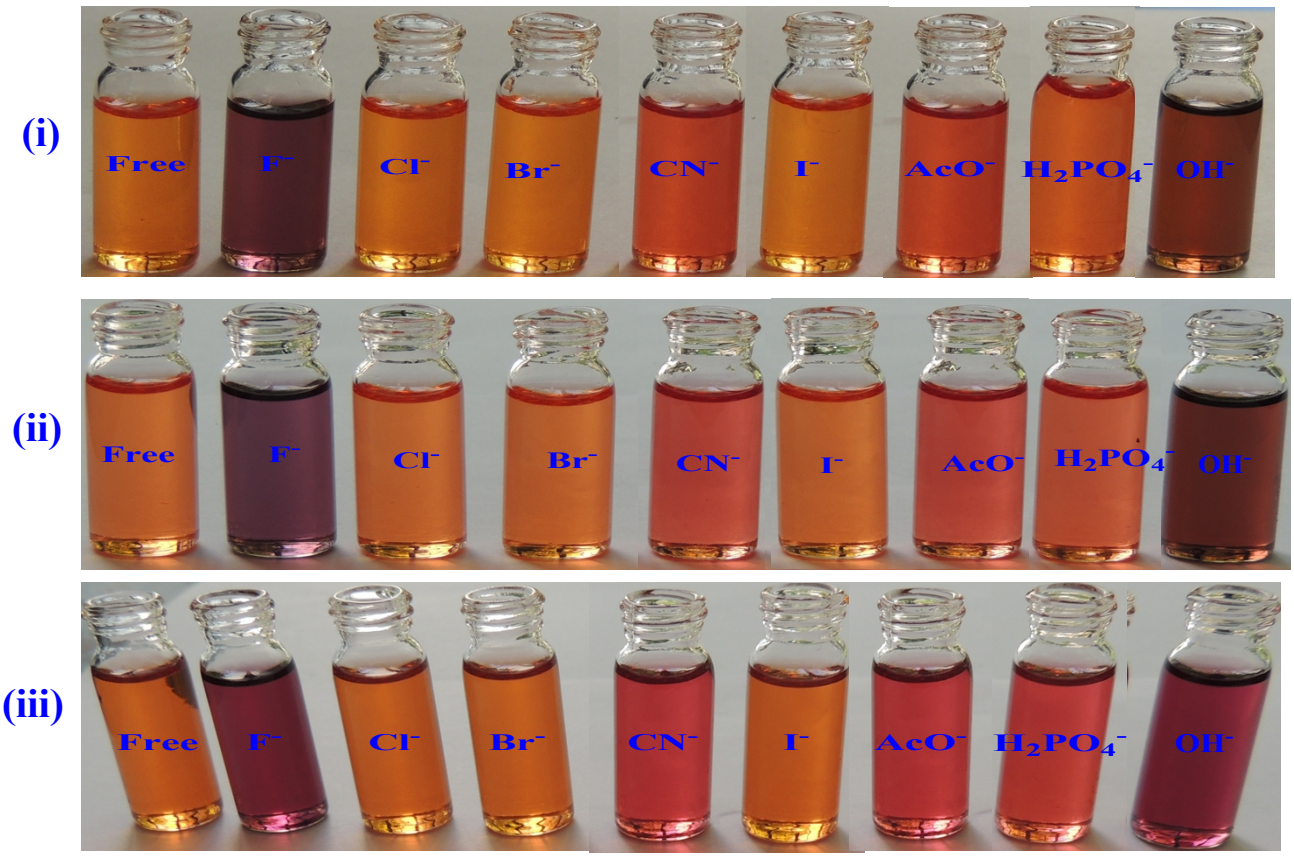

Fig. S2 Color changes that observed when the DMSO solutions of **1** (i), **2** (ii) and **3** (iii) are treated with different anions as their tetrabutylammonium (TBA) salts.

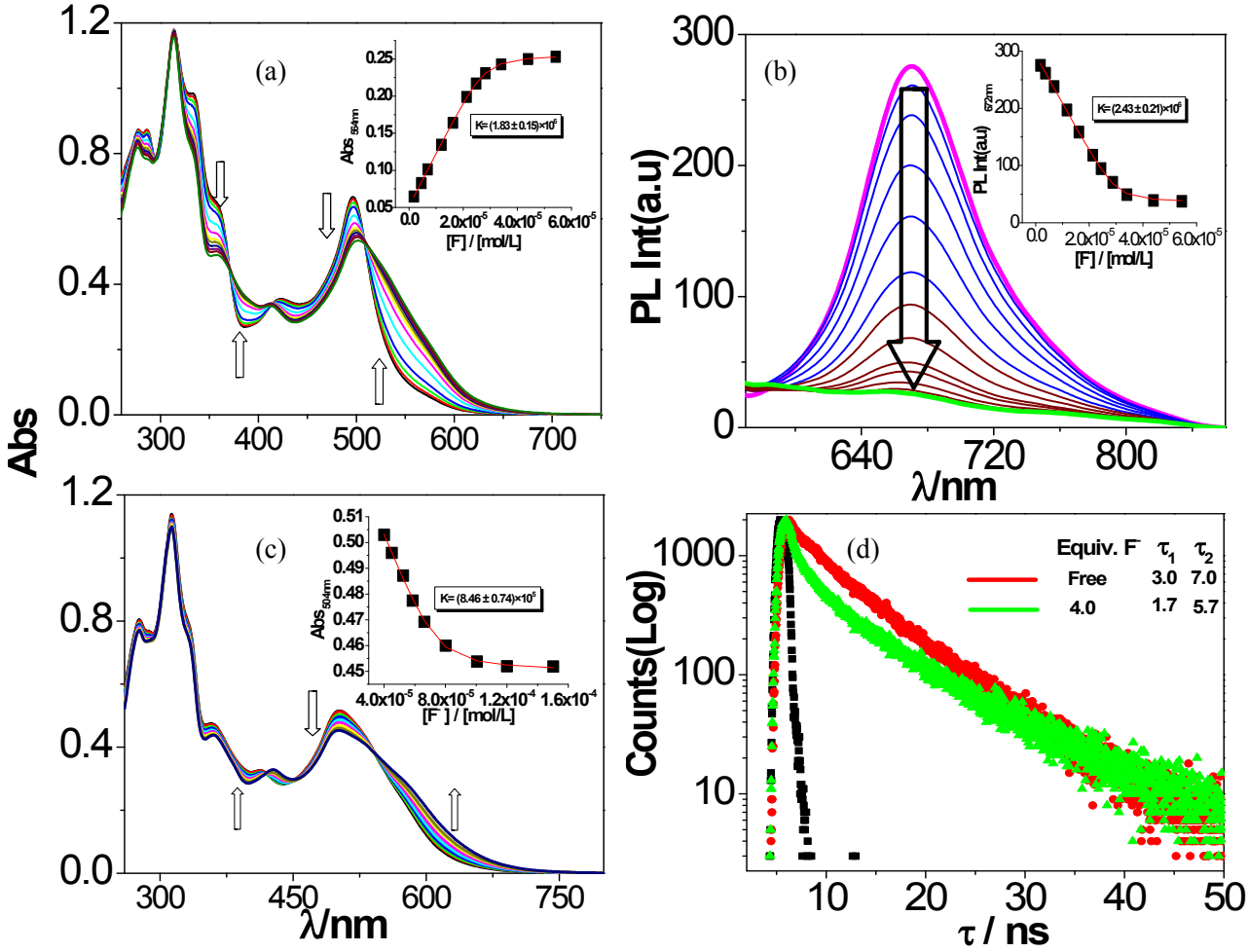

Fig. S3 Changes in UV-vis absorption (a and c), steady state emission (b) spectrum and excited state decay profiles (d) of **1** on incremental addition of F^- in DMSO.

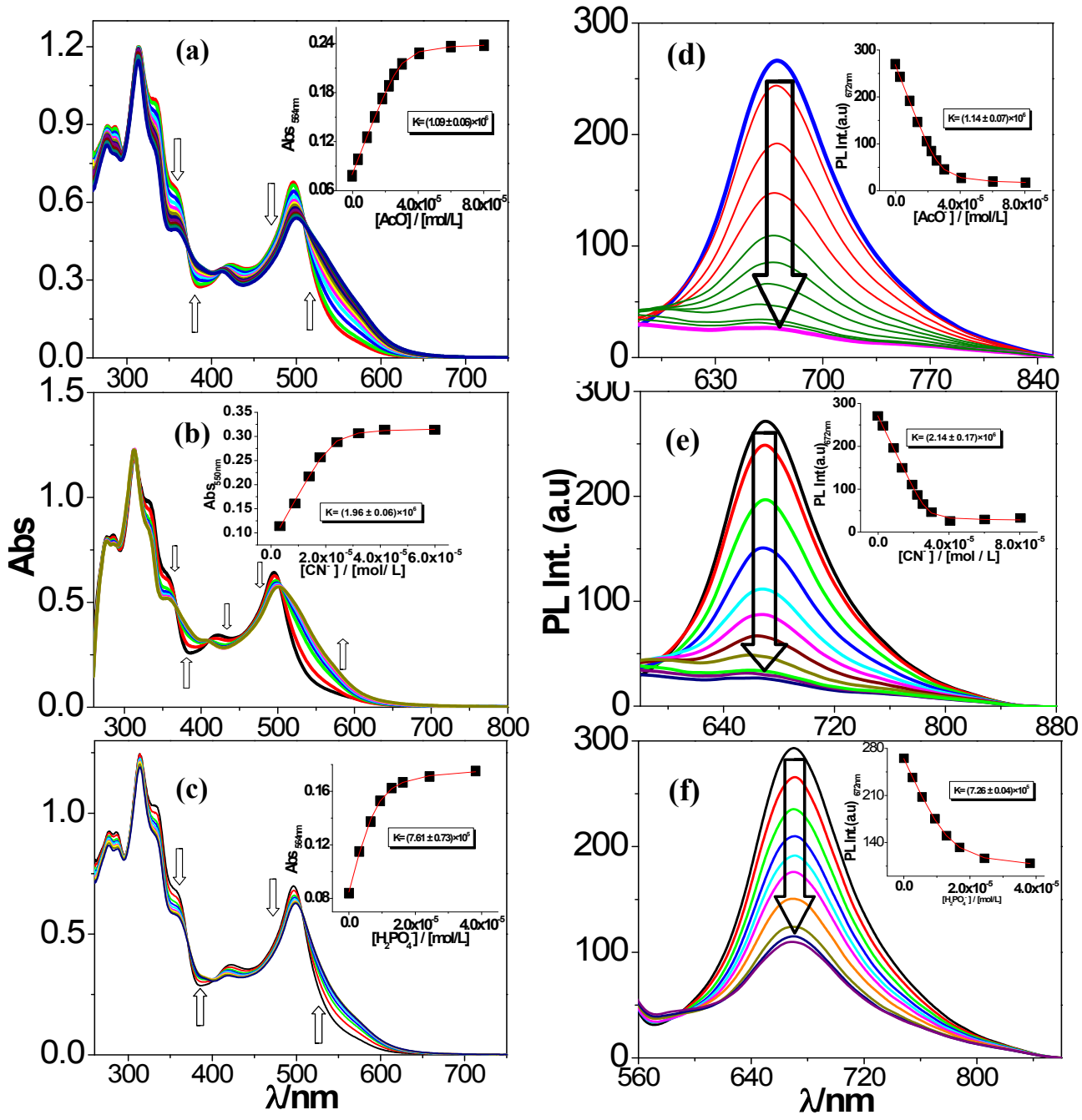

Fig. S4 Changes in UV-vis absorption (a-c) and steady state luminescence (d-f) spectrum of **1** on incremental addition of AcO^-, $CN^-$and $H_2PO_4^-$, respectively in DMSO.

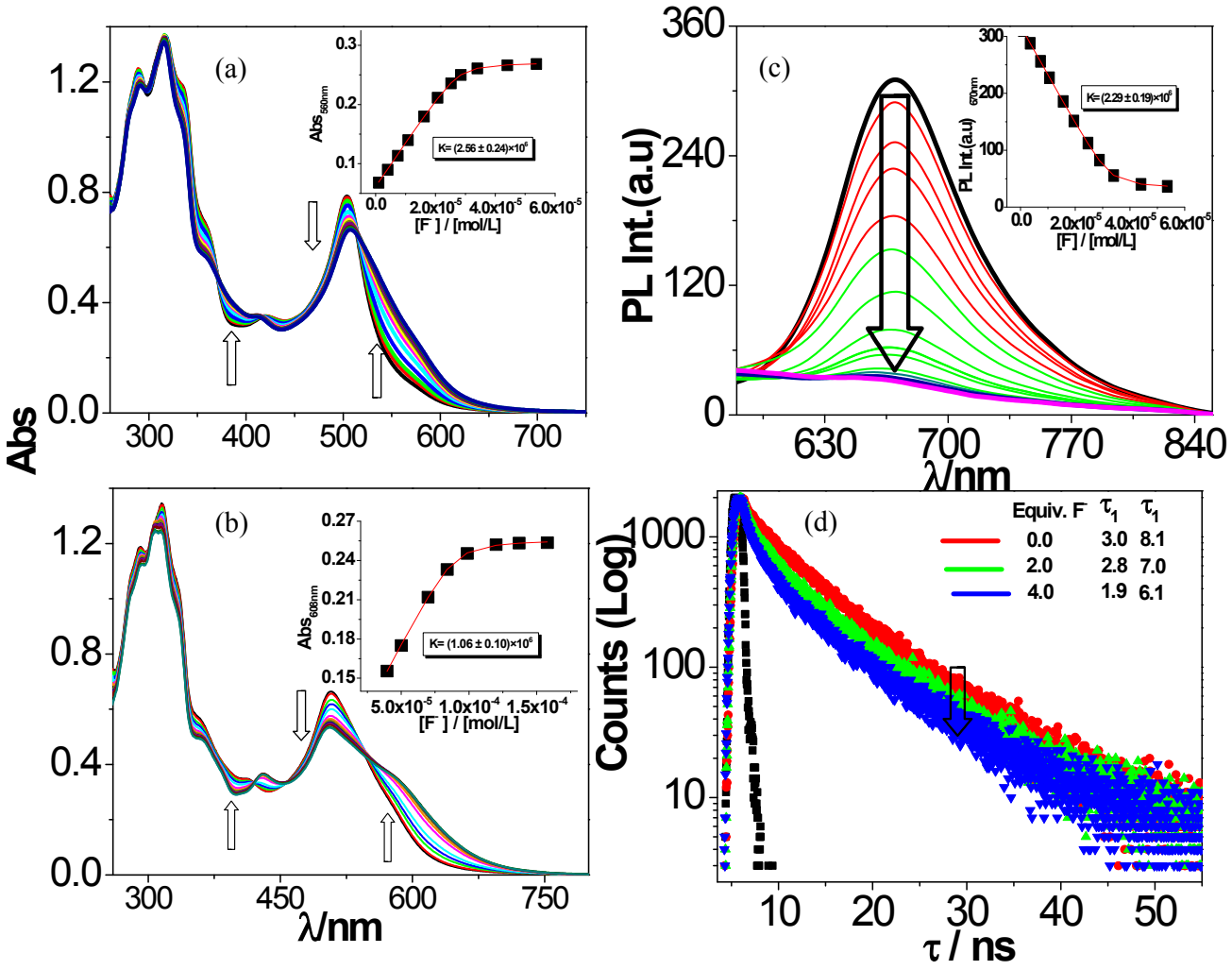

Fig. S5 Changes in UV-vis absorption (a-b), steady state emission (c) spectrum and excited state decay profiles (d) of **2** on incremental addition of F^- in DMSO.

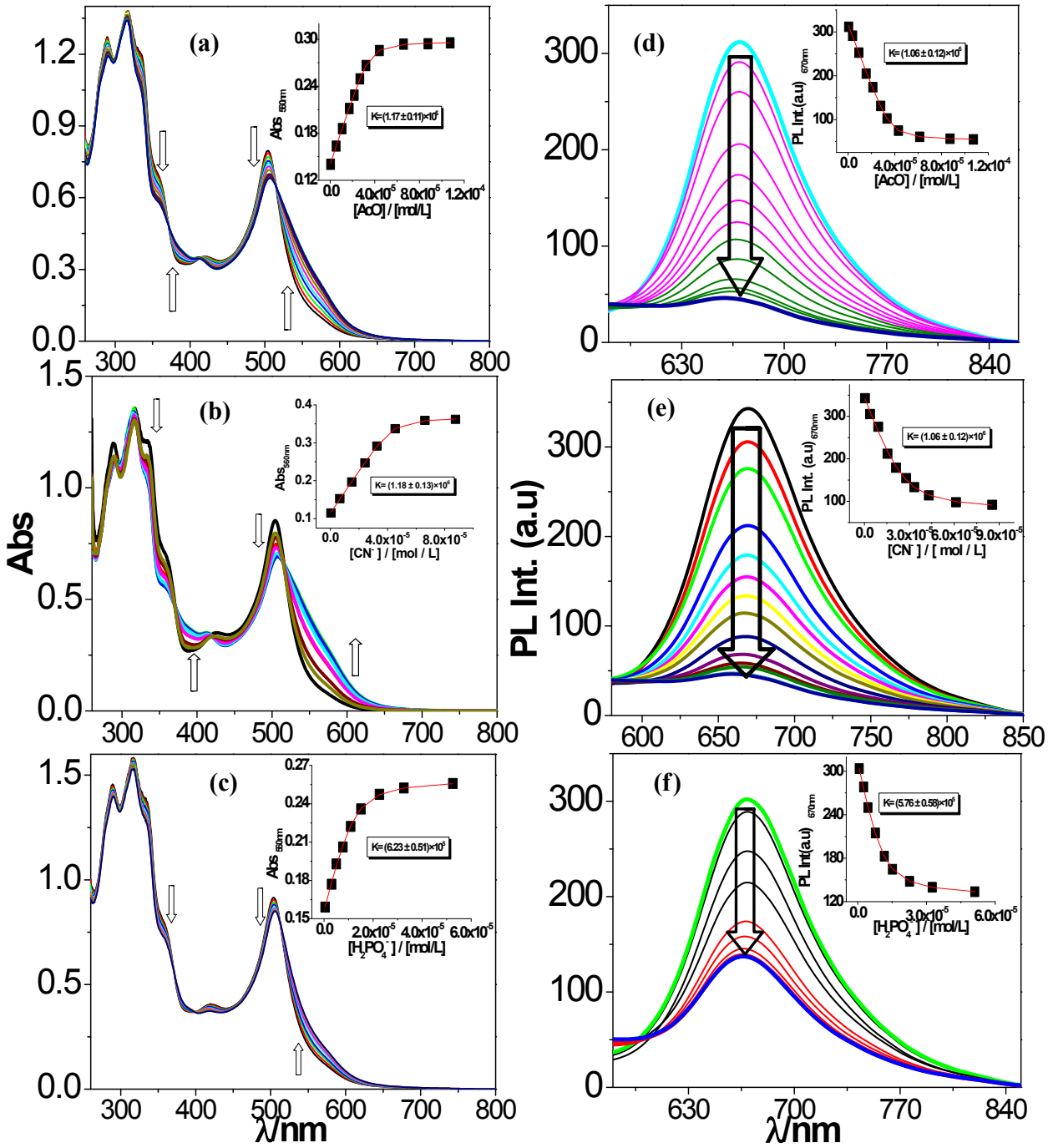

Fig. S6 Changes in UV-vis absorption (a-c) and steady state luminescence (d-f) spectrum of **2** on incremental addition of AcO^-, $CN^-$and $H_2PO_4^-$, respectively in DMSO.

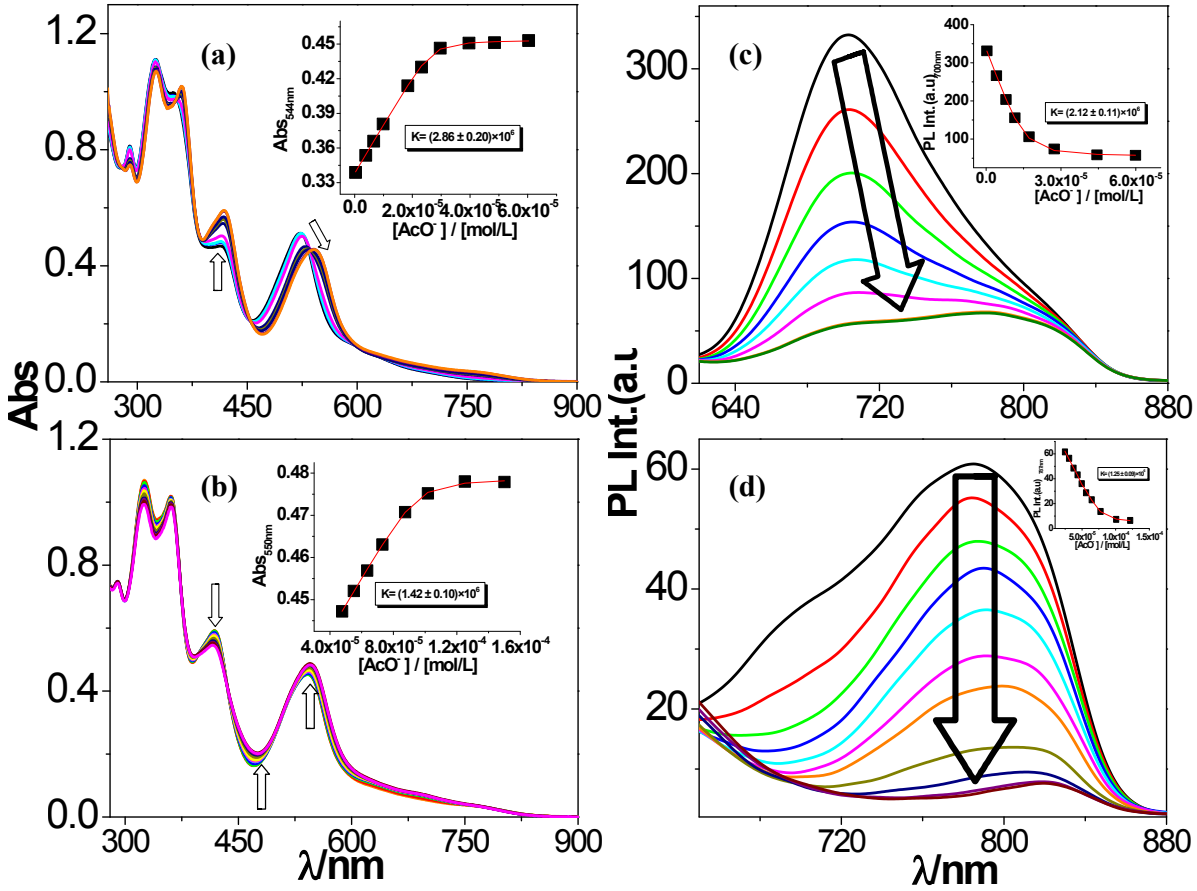

Fig. S7 Changes in UV-vis absorption (a-b) and steady state luminescence (c-d) spectrum of **3** on incremental addition of AcO^- in DMSO.

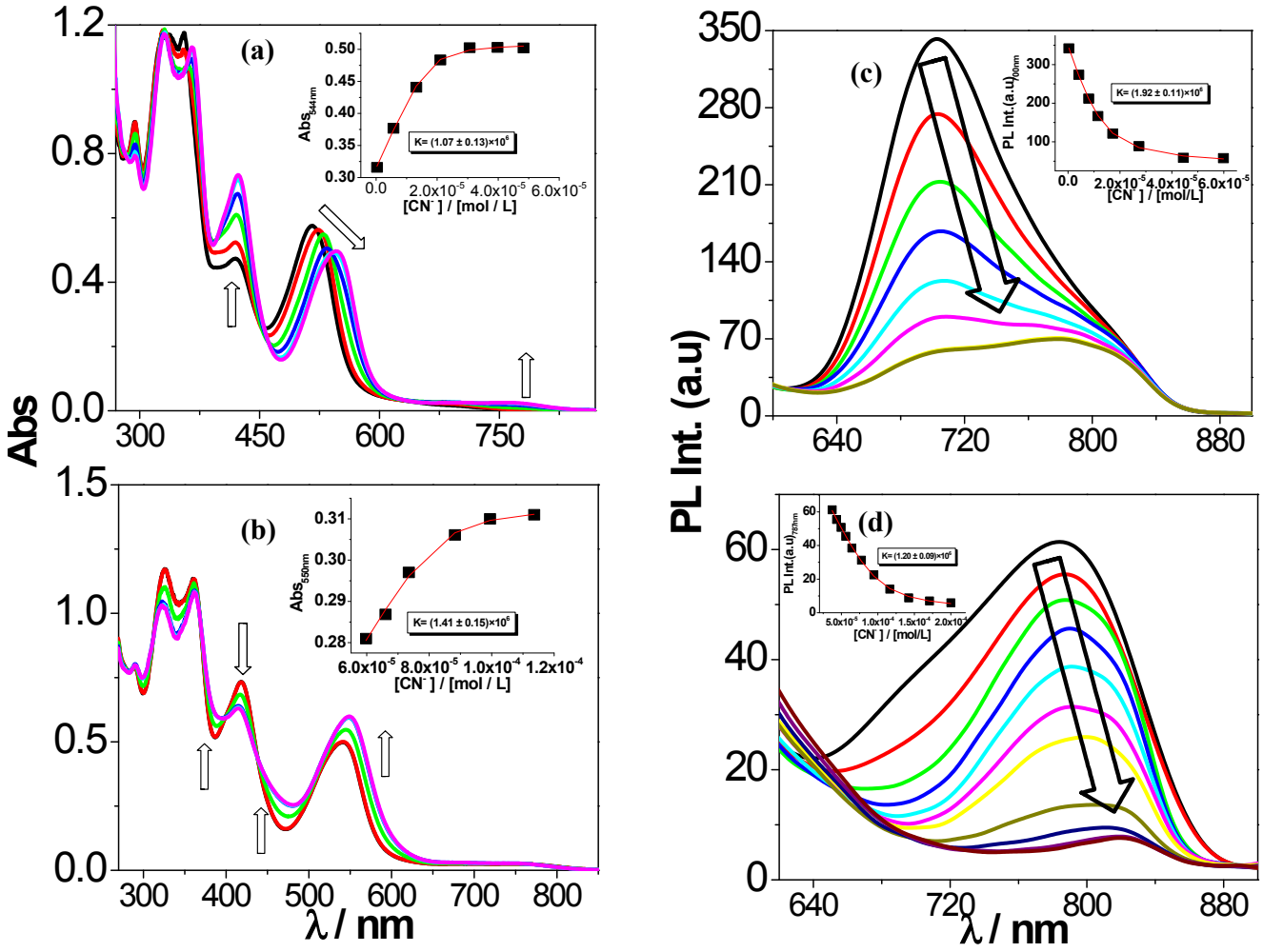

Fig. S8 Changes in UV-vis absorption (a-b) and steady state luminescence (c-d) spectrum of **3** on incremental addition of CN^- in DMSO.

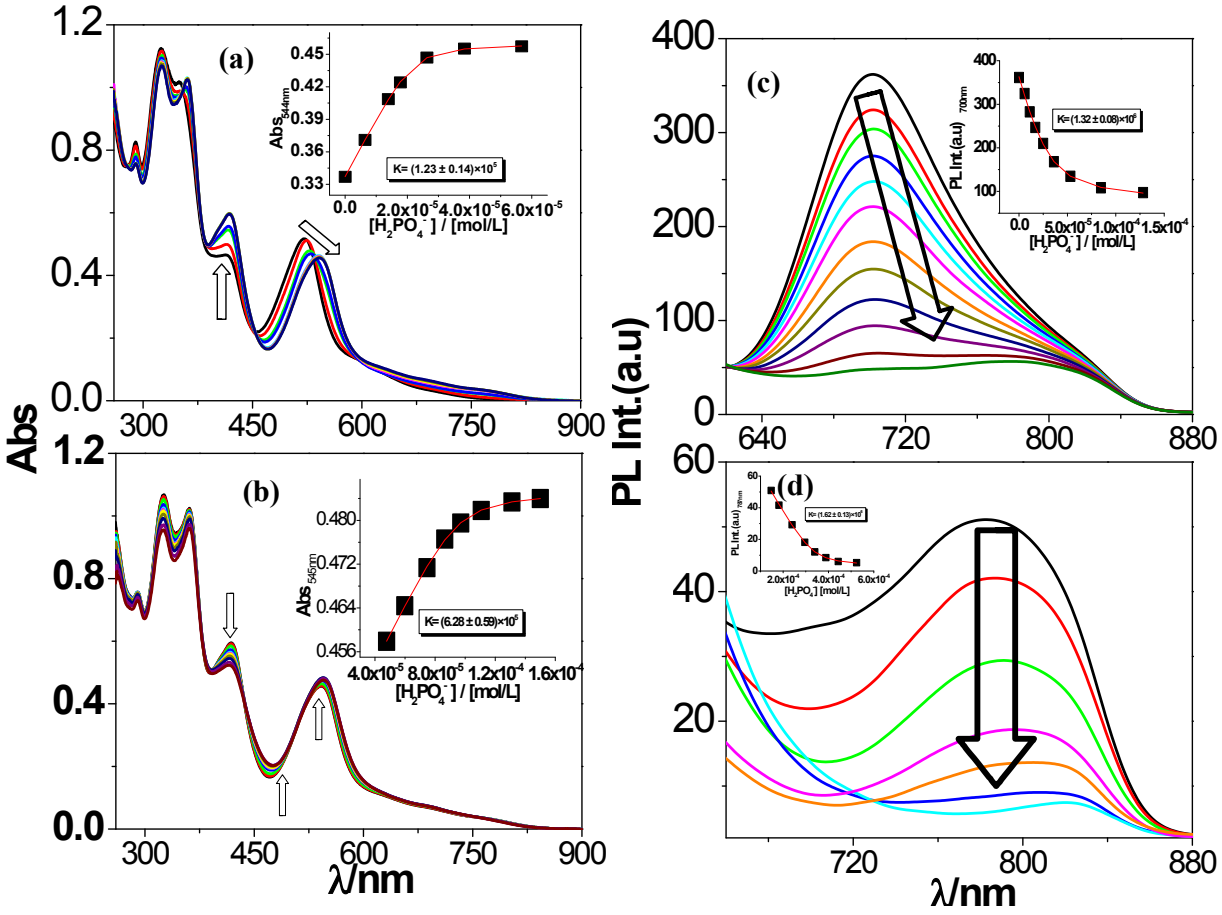

Fig. S9 Changes in UV-vis absorption (a-b) and steady state luminescence (c-d) spectrum of **3** on incremental addition of $H_2PO_4^-$ in DMSO.

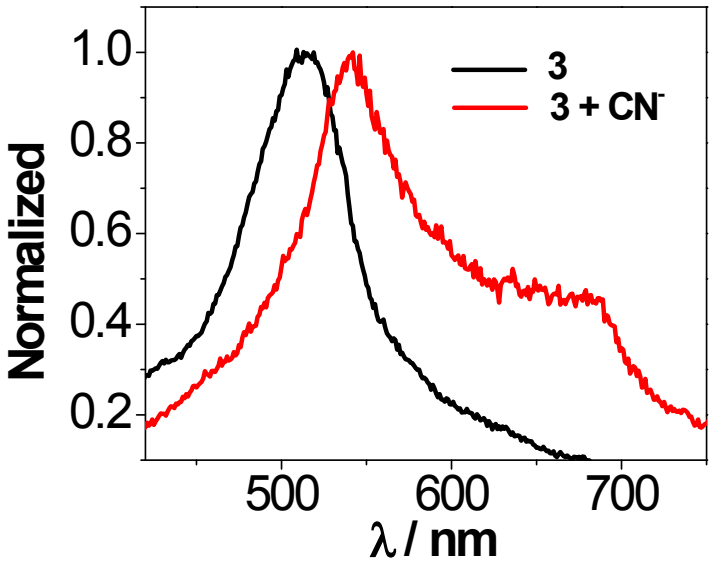

Fig. S10 Normalized luminescence excitation spectrum of **3** before and after the addition of CN^- ion in DMSO. The monitoring emission wavelength is 703 nm and 820 nm, respectively.

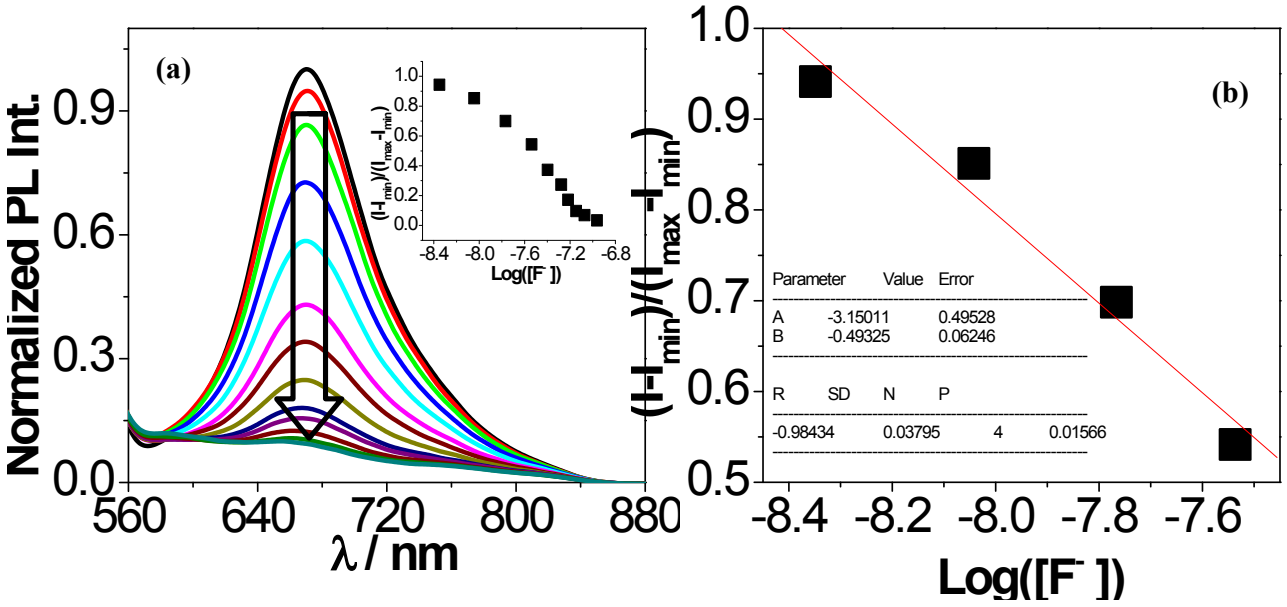

Fig. S11. (a) Photoluminescence changes during the titration of the receptor **1** in DMSO solution, inset: Normalized intensity between the minimum intensity and the maximum intensity. (b) A plot of $(I-I_{min})/(I_{max}-I_{min})$ vs Log([F^-]), the calculated detection limit of receptor is 3.89×10^{-9}M.

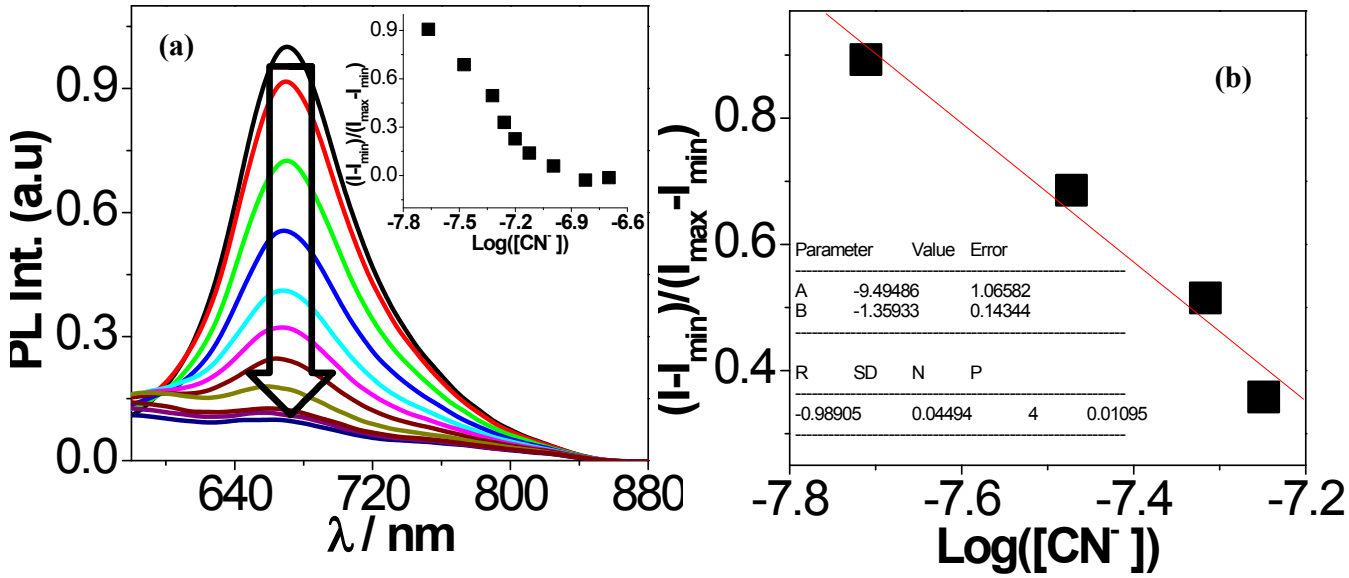

Fig. S12 (a) Photoluminescence changes during the titration of the receptor **1** in DMSO solution, inset: Normalized intensity between the minimum intensity and the maximum intensity. (b) A plot of $(I-I_{min})/(I_{max}-I_{min})$ vs Log([CN^-]), the calculated detection limit of receptor is 1.72×10^{-8}M.

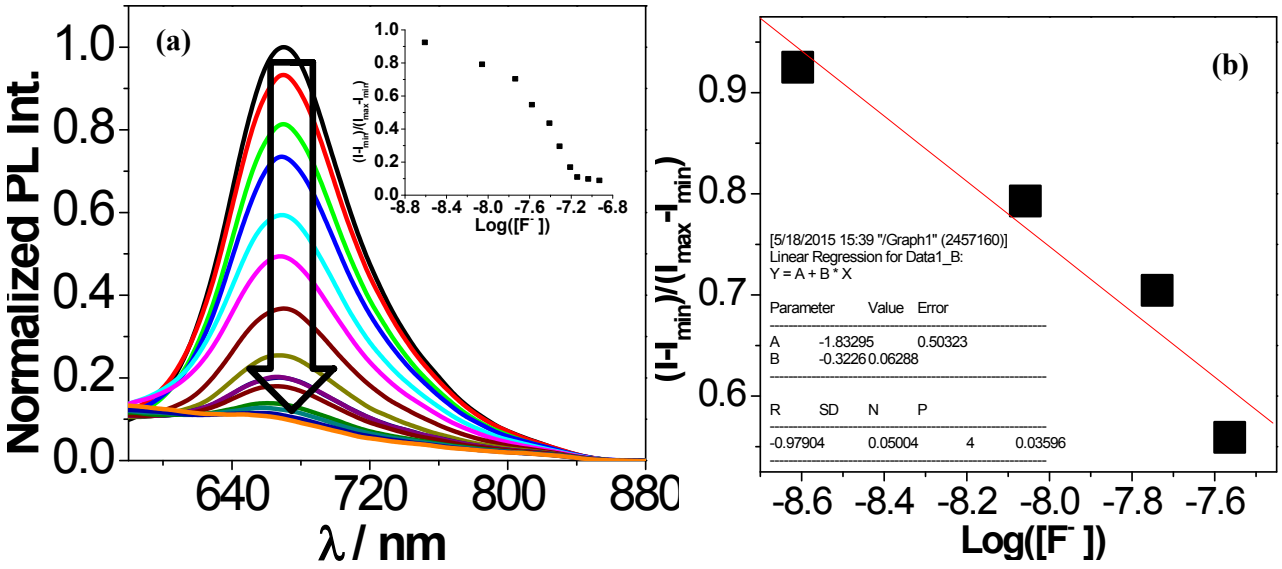

Fig. S13 (a) Photoluminescence changes during the titration of the receptor **2** in DMSO solution, inset: Normalized intensity between the minimum intensity and the maximum intensity. (b) A plot of $(I-I_{min})/(I_{max}-I_{min})$ vs Log([F^-]), the calculated detection limit of receptor is 1.97×10^{-9}M.

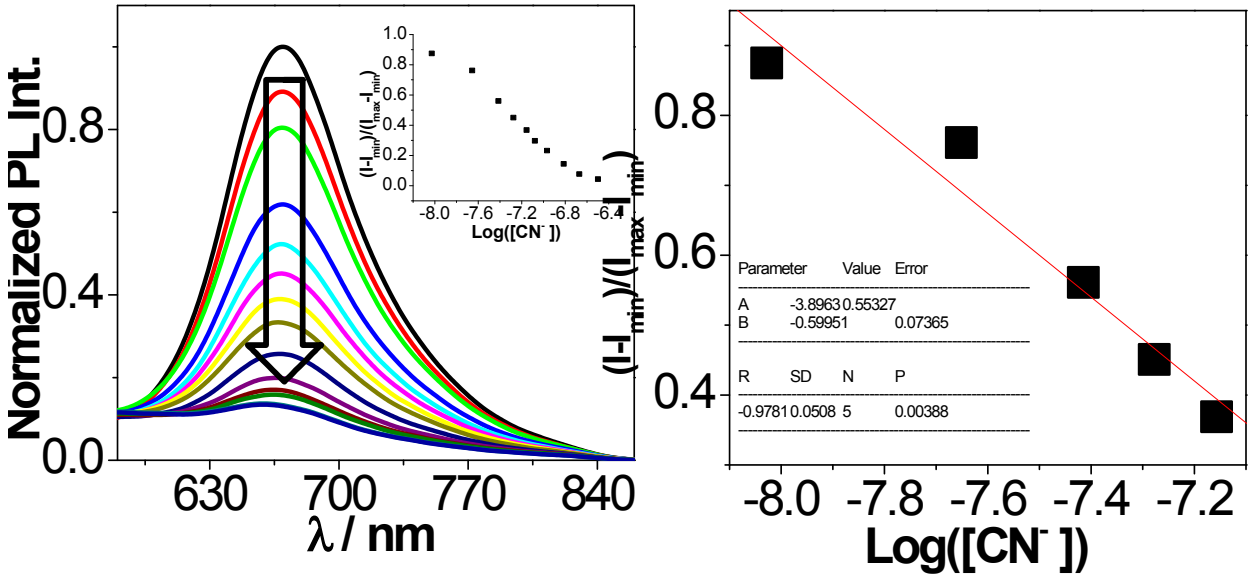

Fig. S14 (a) Photoluminescence changes during the titration of the receptor **2** in DMSO solution, inset: Normalized intensity between the minimum intensity and the maximum intensity. (b) A plot of $(I-I_{min})/(I_{max}-I_{min})$ vs Log([CN^-]), the calculated detection limit of receptor is 8.51×10^{-9} M.

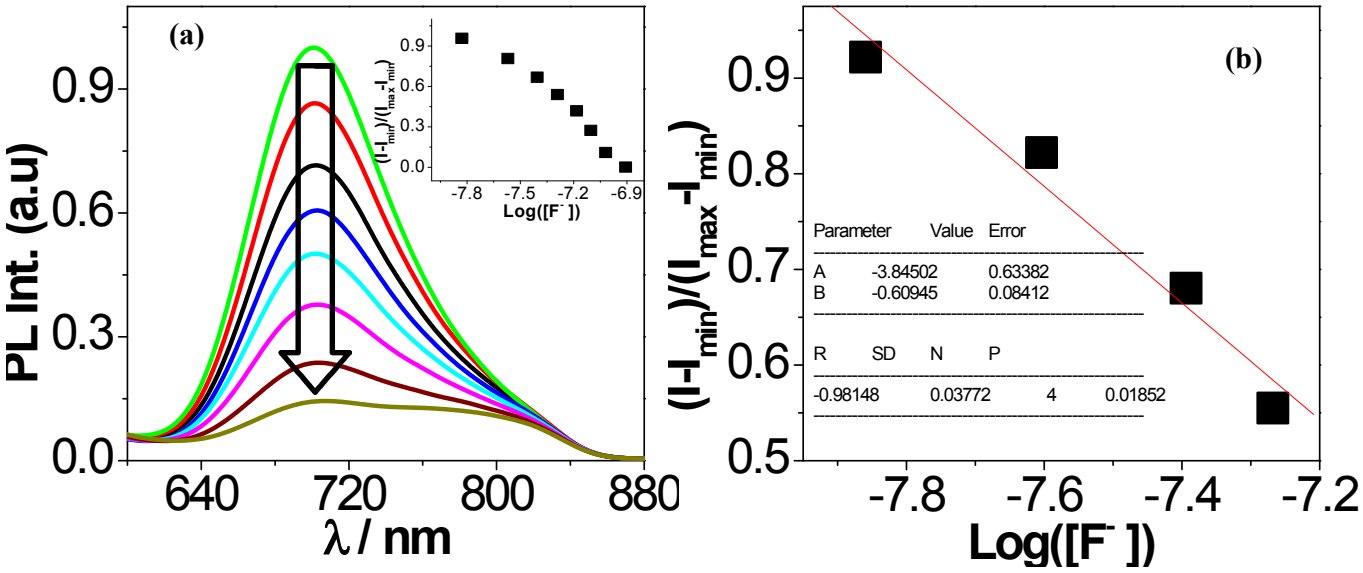

Fig. S15 (a) Photoluminescence changes during the titration of the receptor **3** in DMSO solution, inset: Normalized intensity between the minimum intensity and the maximum intensity. (b) A plot of $(I-I_{min})/(I_{max}-I_{min})$ vs Log([F^-]), the calculated detection limit of receptor is 1.23×10^{-8}M.

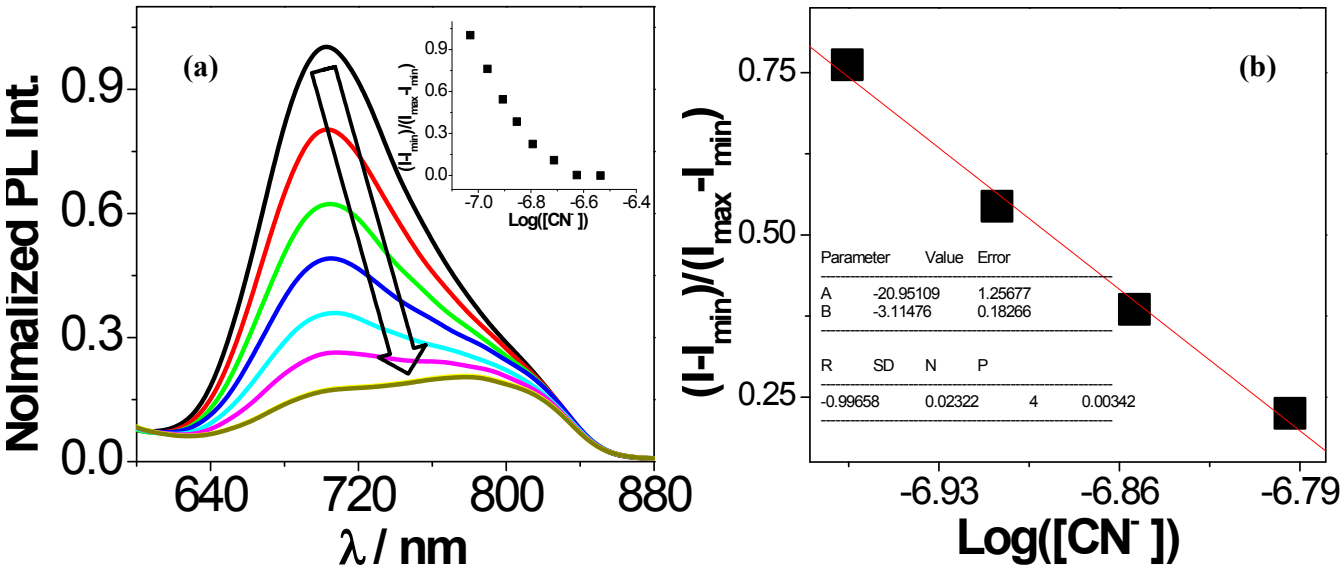

Fig. S16 (a) Photoluminescence changes during the titration of the receptor **3** in DMSO solution, inset: Normalized intensity between the minimum intensity and the maximum intensity. (b) A plot of $(I-I_{min})/(I_{max}-I_{min})$ vs Log([CN^-]), the calculated detection limit of receptor is 1.04×10^{-7} M.

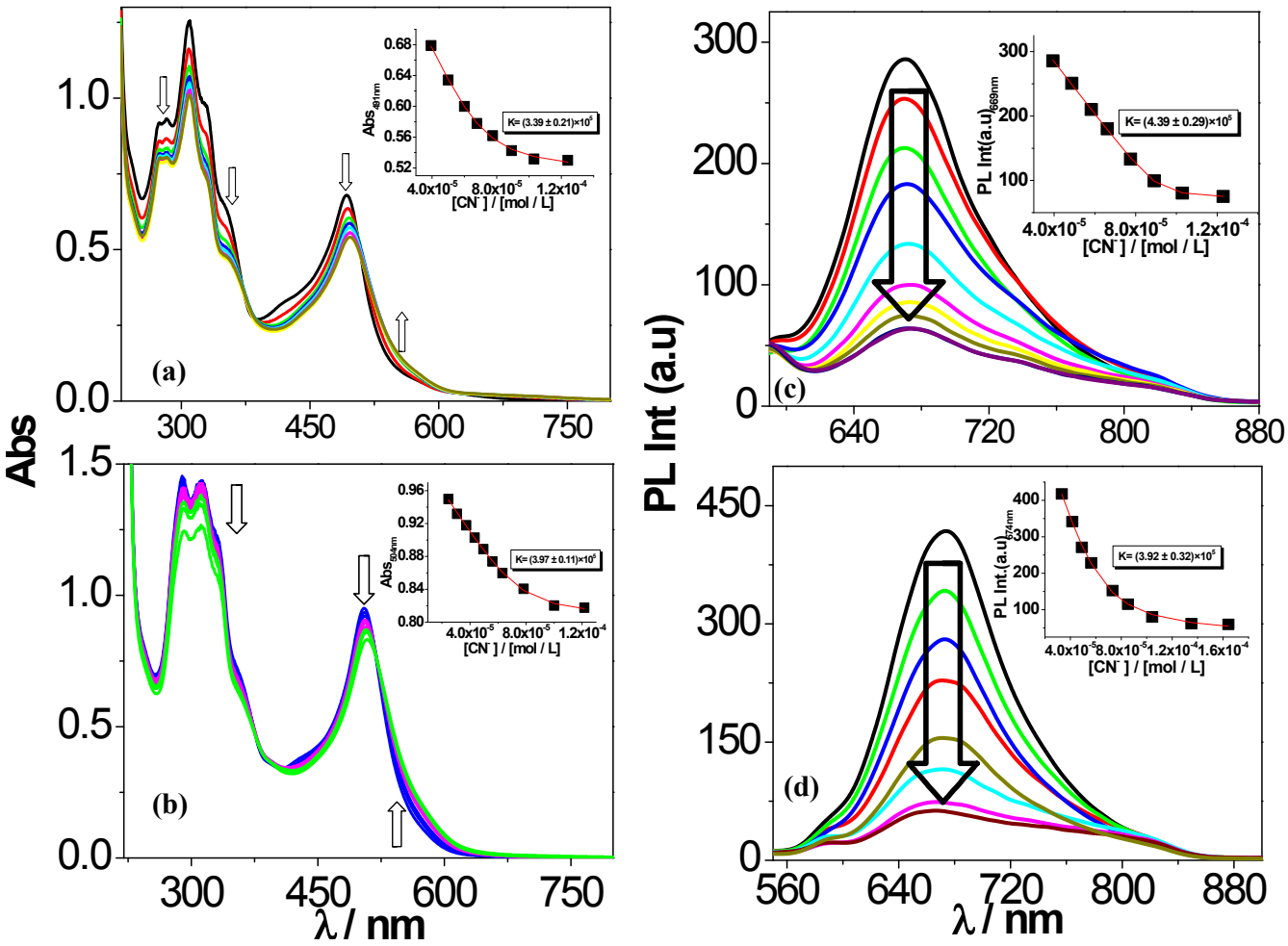

Fig. S17 Changes in UV-vis absorption (a-b) and steady state luminescence (c-d) spectrum of **1** and **2,** respectively on incremental addition of CN^- in DMSO-H_2O (1:100).

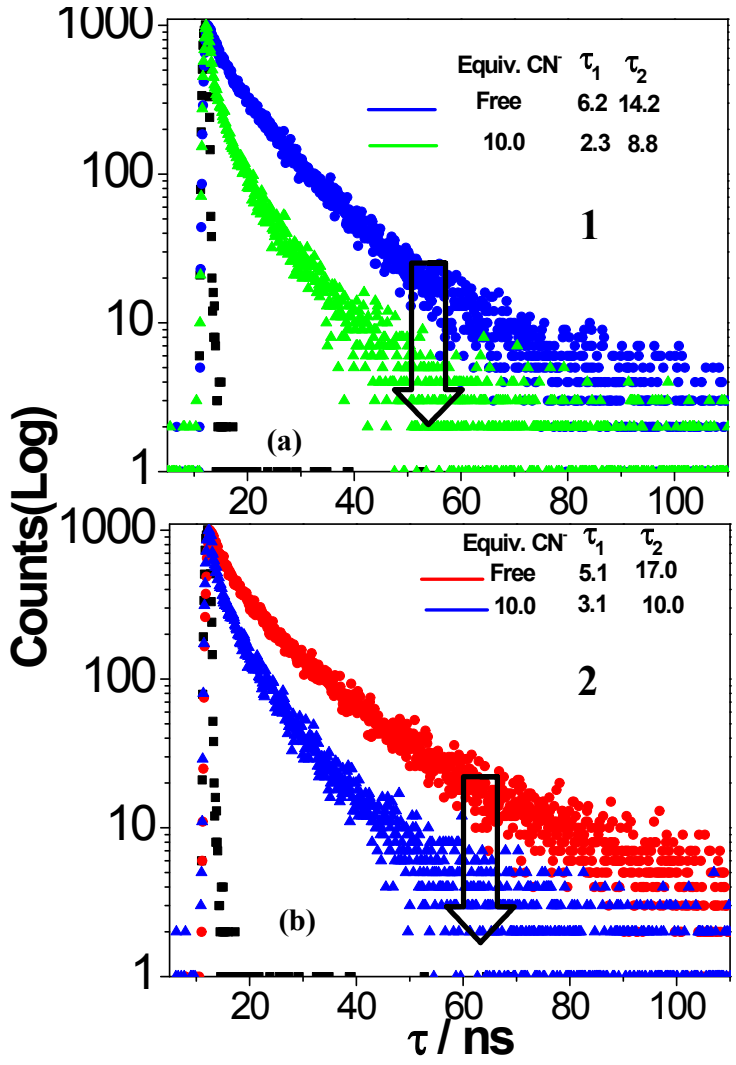

Fig. 18 Changes in time-resolved luminescence spectra (a and b) of **1** and **2**, respectively in DMSO-H_2O (1:100) upon addition of CN^- anions as TBA salts.

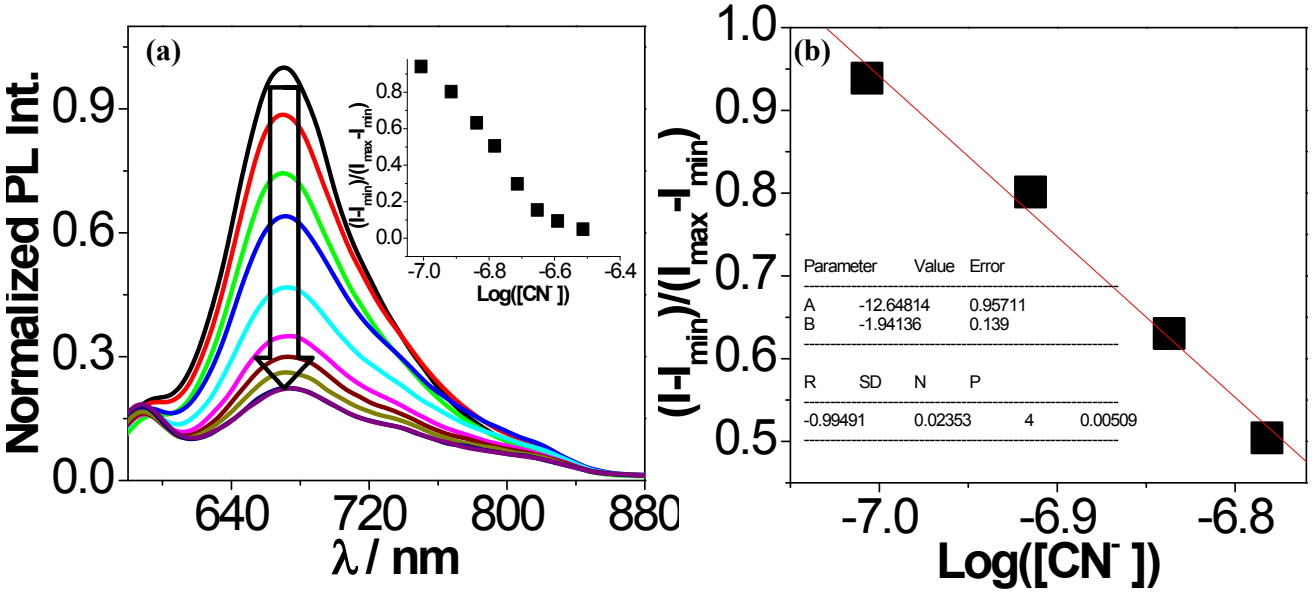

Fig. S19 (a) Photoluminescence changes during the titration of the receptor **1** in DMSO-H_2O (1:100) solution, inset: Normalized intensity between the minimum intensity and the maximum intensity. (b) A plot of $(I-I_{min})/(I_{max}-I_{min})$ vs Log([CN^-]), the calculated detection limit of receptor is 9.31×10^{-8} M.

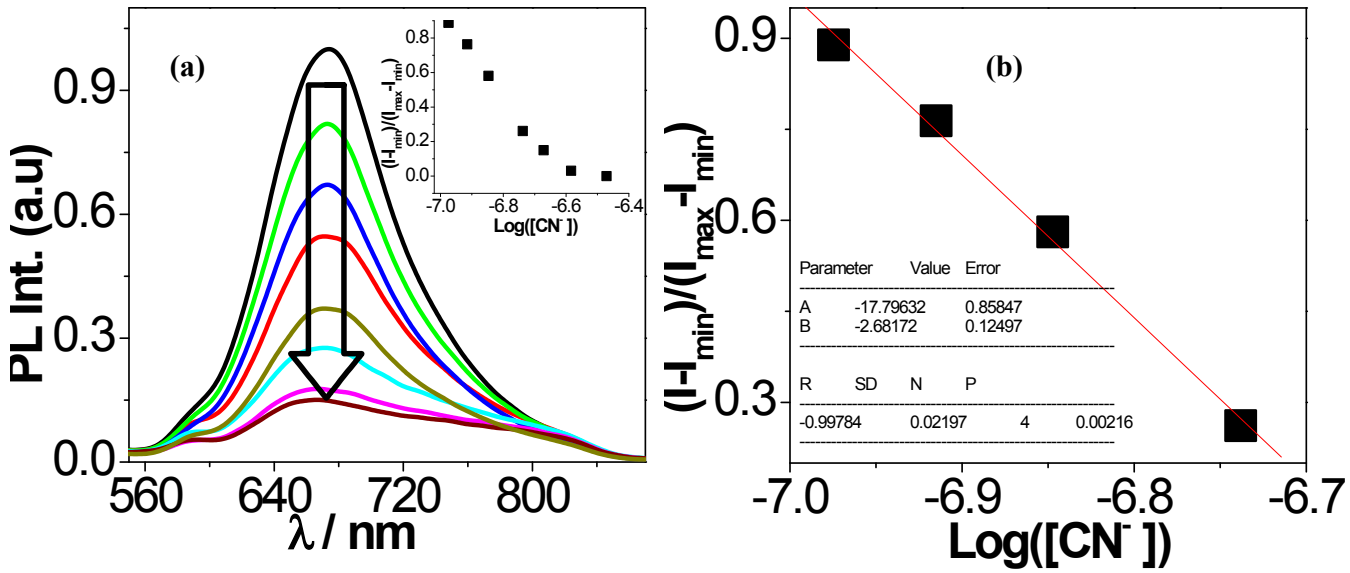

Fig. S20 (a) Photoluminescence changes during the titration of the receptor **2** in DMSO-H_2O (1:100) solution, inset: Normalized intensity between the minimum intensity and the maximum intensity. (b) A plot of $(I-I_{min})/(I_{max}-I_{min})$ vs Log([CN^-]), the calculated detection limit of receptor is 10.19×10^{-8} M.

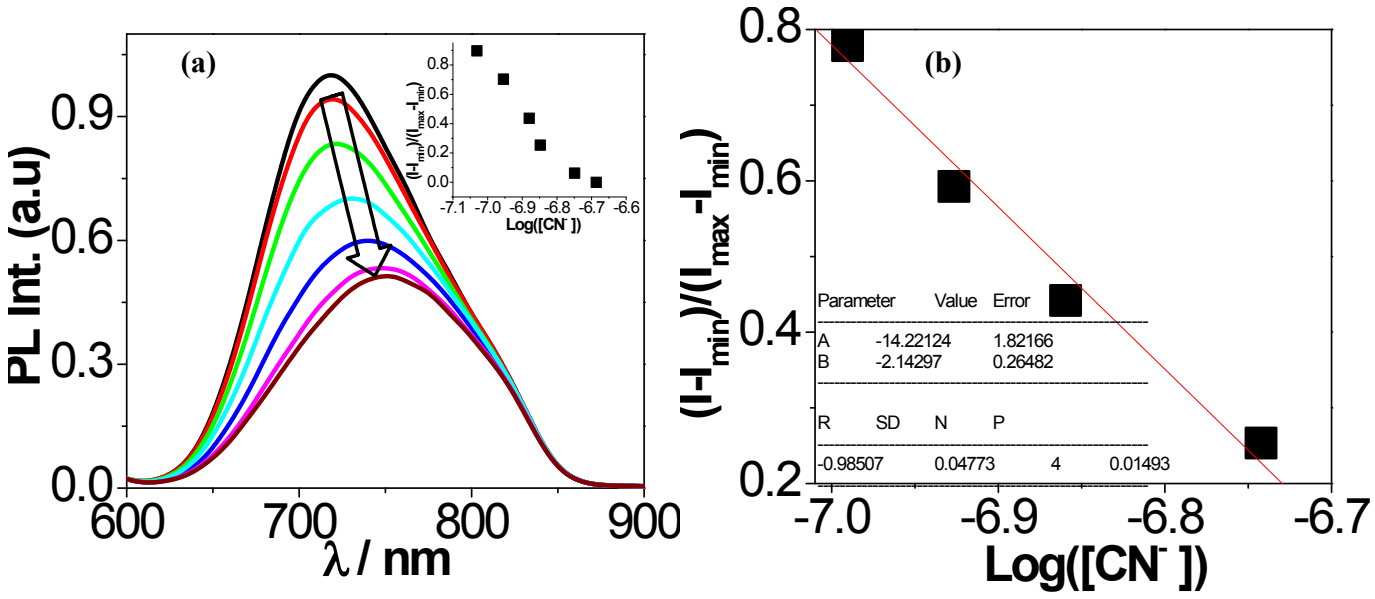

Fig. S21 (a) Photoluminescence changes during the titration of the receptor **3** in DMSO-H_2O (1:100) solution, inset: Normalized intensity between the minimum intensity and the maximum intensity. (b) A plot of $(I-I_{min})/(I_{max}-I_{min})$ vs Log([CN^-]), the calculated detection limit of receptor is 9.79×10^{-8} M.

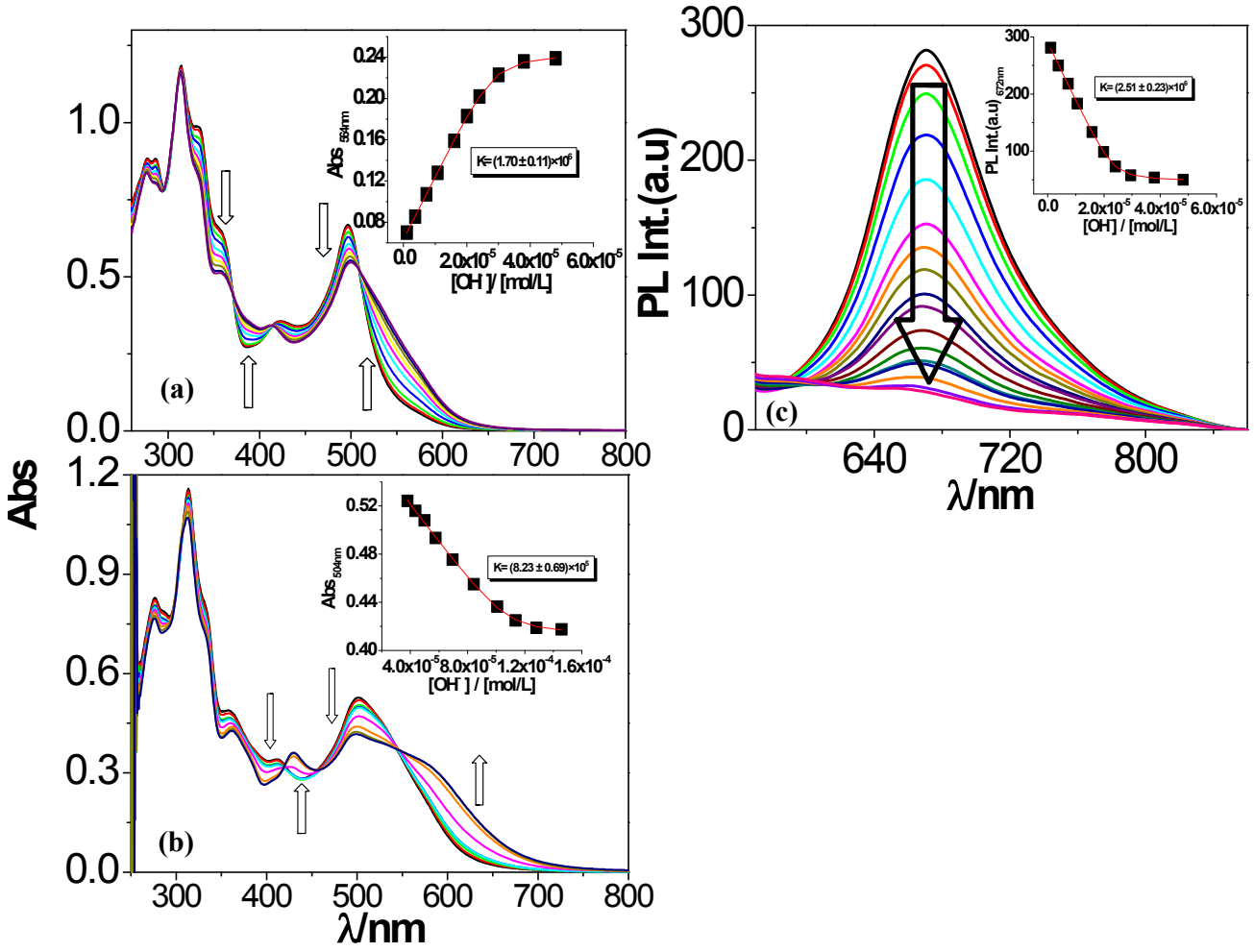

Fig. S22 Changes in UV-vis absorption (a-b) and steady state luminescence (c) spectrum of **1** on incremental addition of OH^- in DMSO.

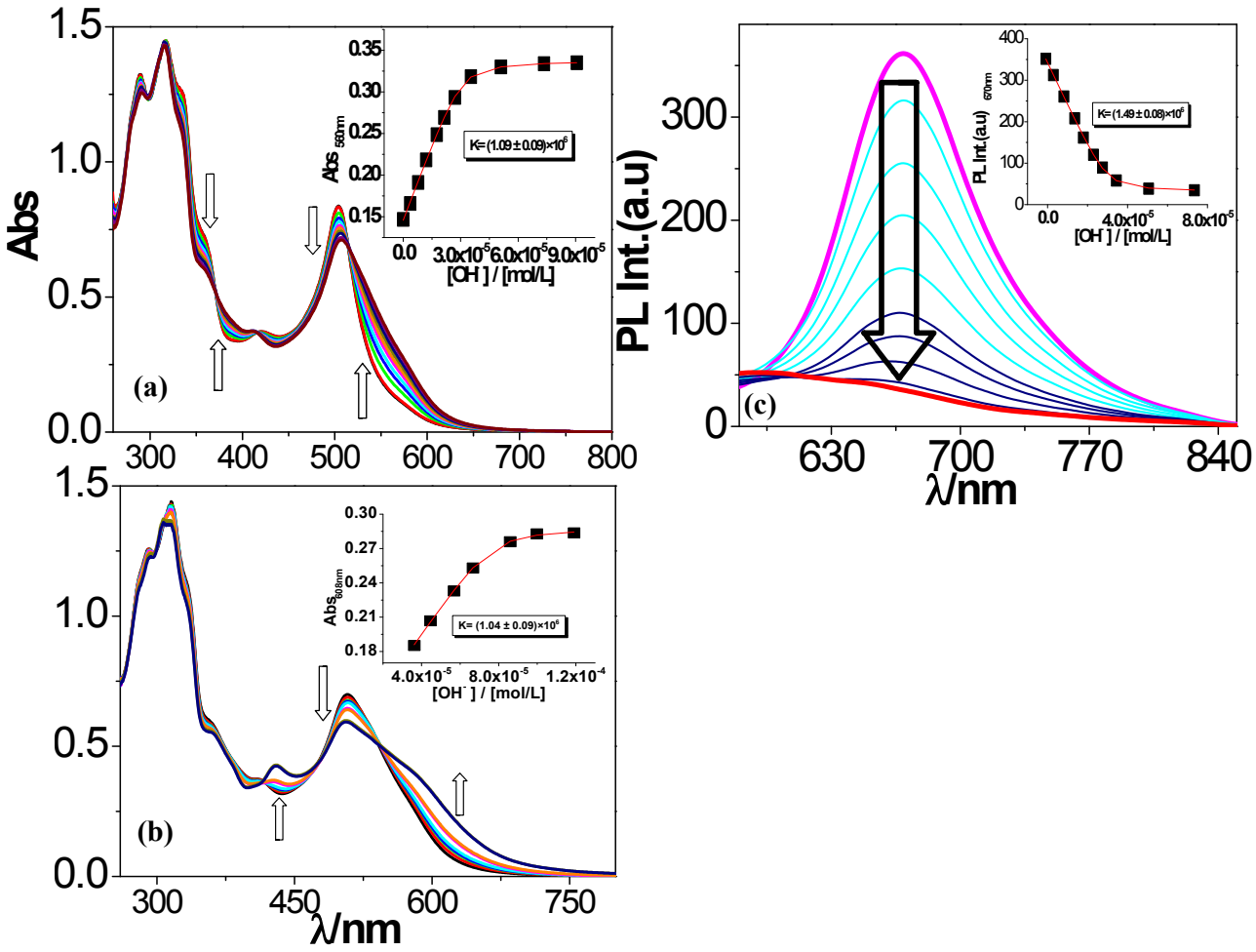

Fig. S23 Changes in UV-vis absorption (a-b) and steady state luminescence (c) spectrum of **2** on incremental addition of OH^- in DMSO.

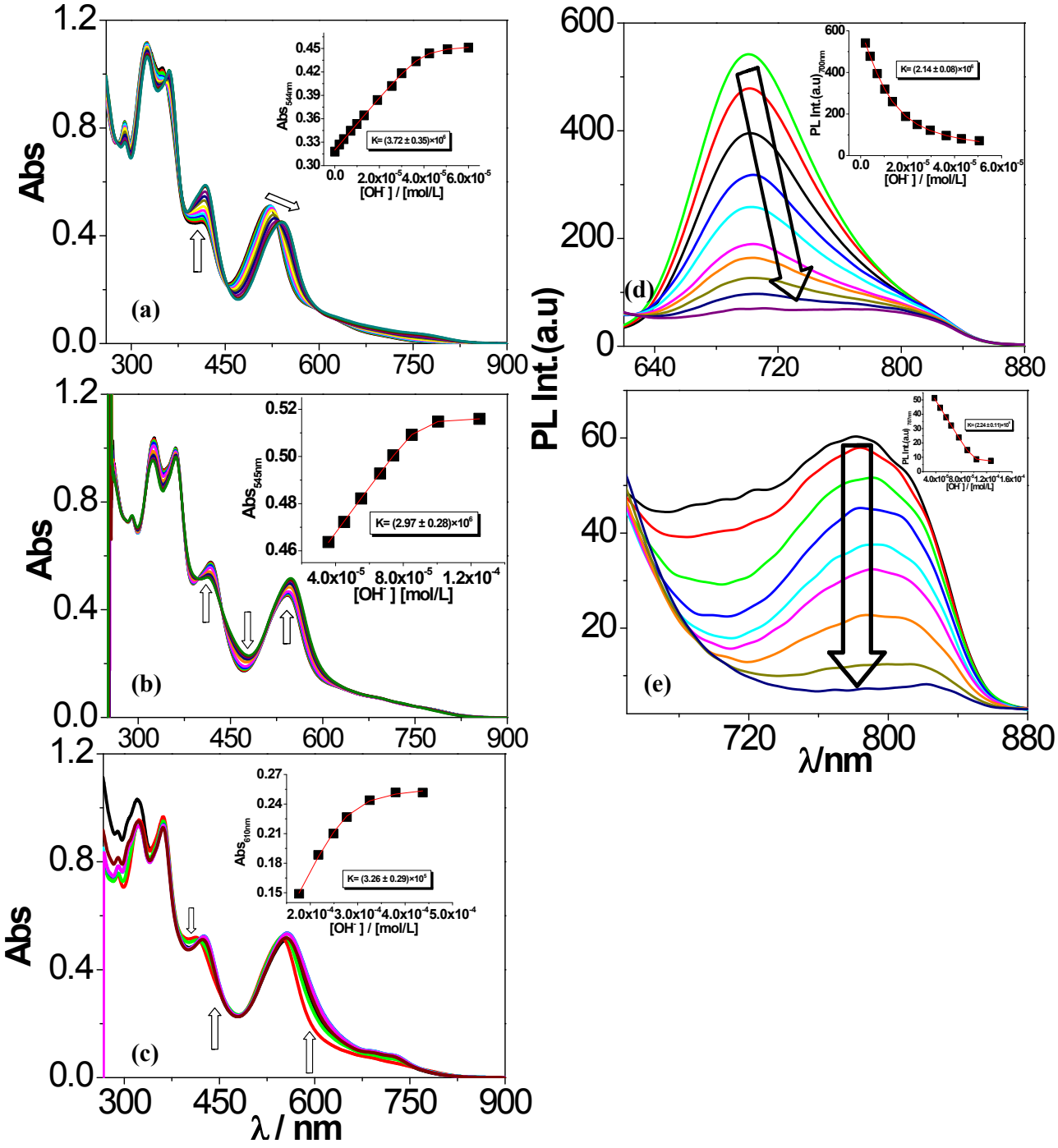

Fig. S24 Changes in UV-vis absorption (a-c) and steady state luminescence (d-e) spectrum of **3** on incremental addition of OH^- in DMSO.

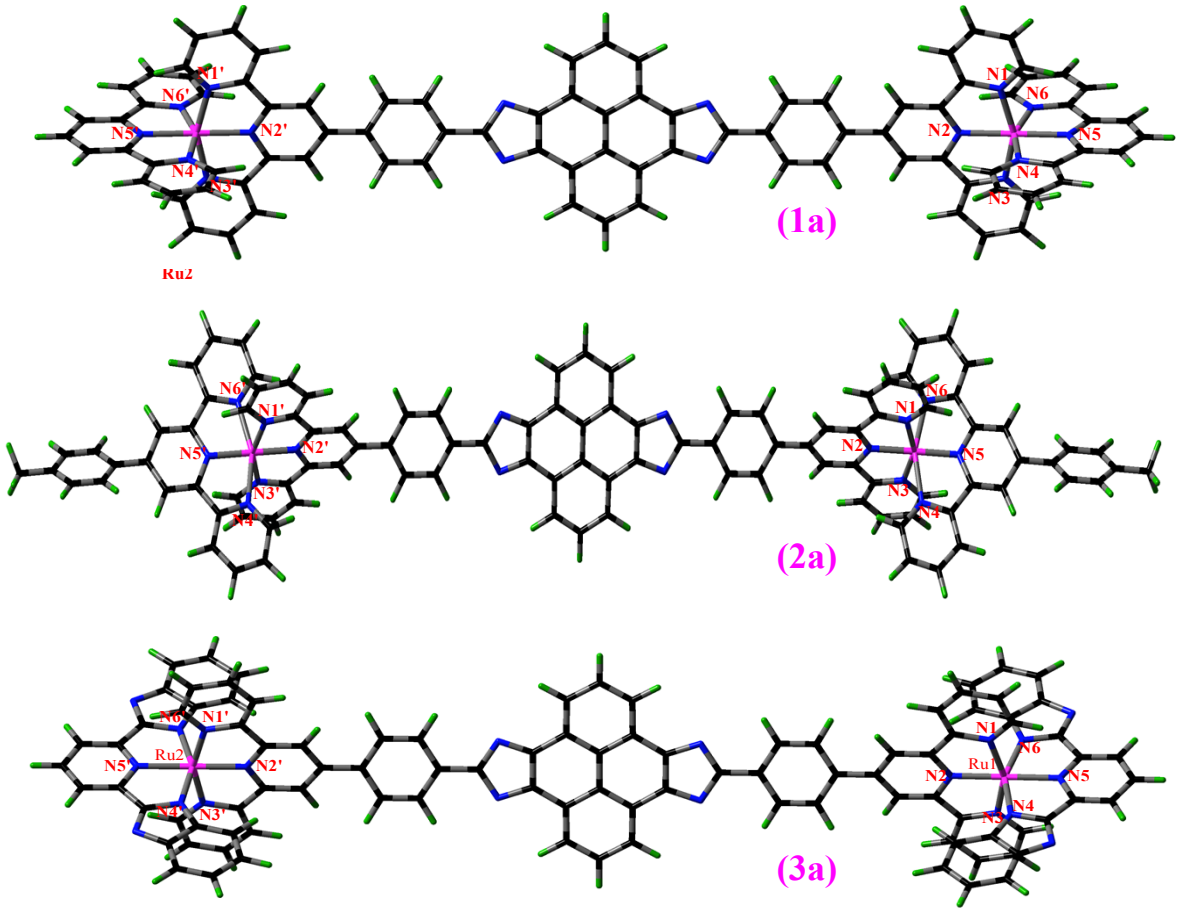

Fig. S25 Optimized geometries and labeling schemes of [(tpy)Ru(tpy-PhImzPy-tpy)Ru (tpy)]$^{2+}$ (**1a**), [(tpy-PhCH$_3$)Ru(tpy-PhImzPy-tpy)Ru(tpy-PhCH$_3$)]$^{2+}$ **(2a)** and [(pbbzim)Ru (tpy-PhImzPy-tpy)Ru(pbbzim)]$^{2-}$ (**3a**) in DMSO.

	Hole	Electron
1a 450 nm S_{37} ff = 0.52	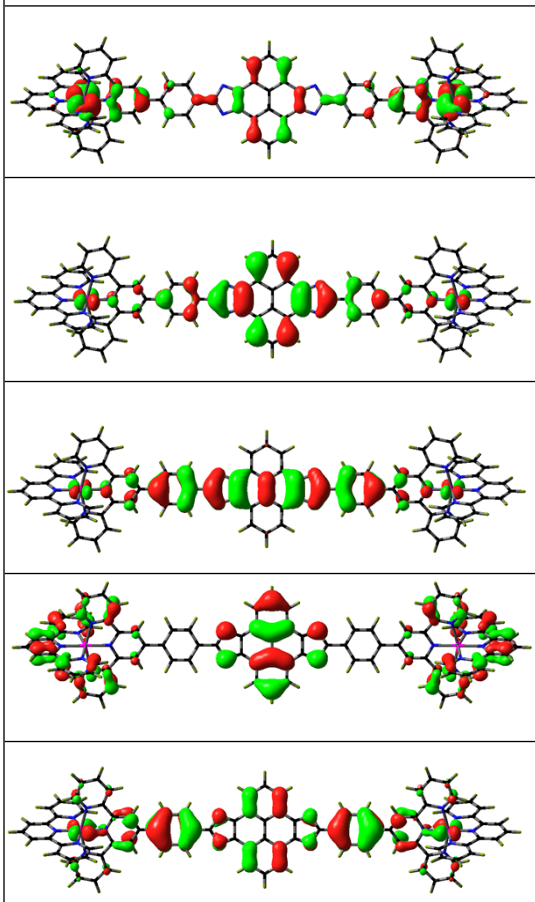	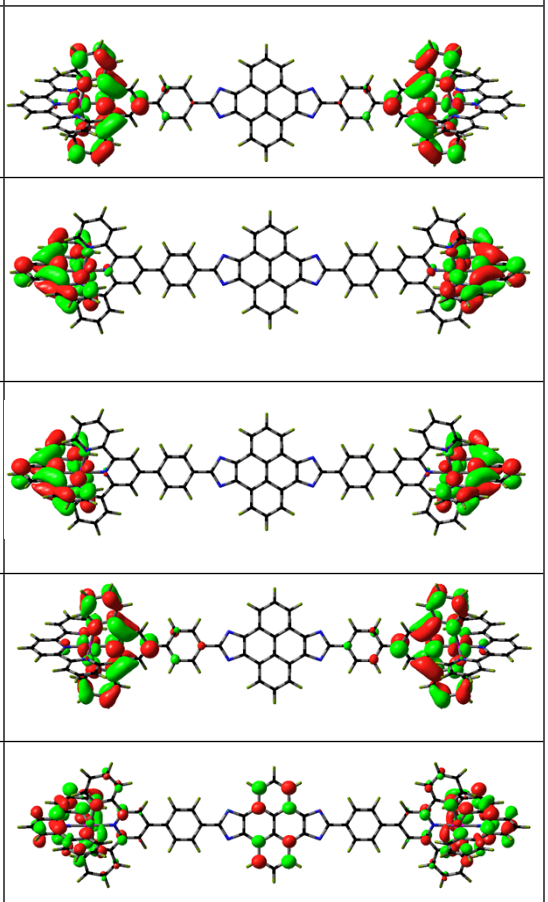

Fig. S26 NTOs illustrating the nature of optically active singlet excited states in the absorption bands at 450 nm for **1a**. The occupied (holes) and unoccupied (electrons) NTO pairs that contribute more than 10 % to each excited state are only represented.

2a 459 nm S_{37} f = 0.60	Hole	Electron
	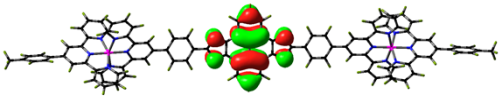	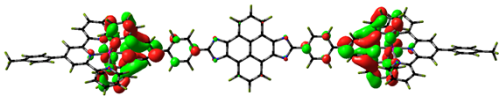
	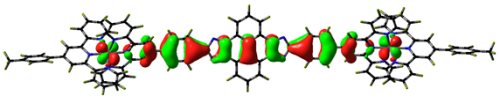	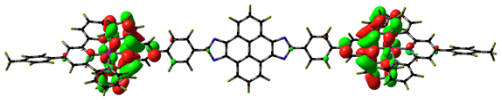
	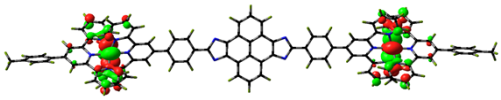	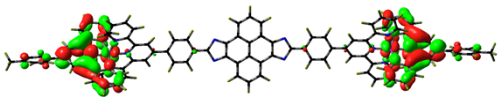

Fig. S27 NTOs illustrating the nature of optically active singlet excited states in the absorption bands at 459 nm for **2a**. The occupied (holes) and unoccupied (electrons) NTO pairs that contribute more than 10 % to each excited state are only represented.

3a 551 nm S_{11} f = 0.70	Hole	Electron
	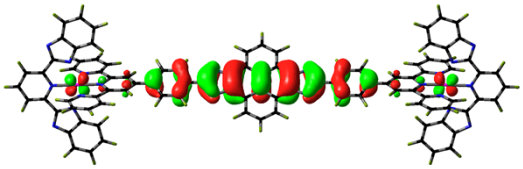	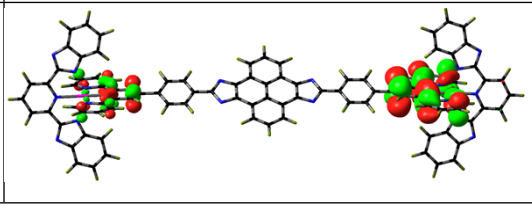

Fig. S28 NTOs illustrating the nature of optically active singlet excited states in the absorption bands at 551 nm for **3a**. The occupied (holes) and unoccupied (electrons) NTO pairs that contribute more than 10 % to each excited state are only represented.

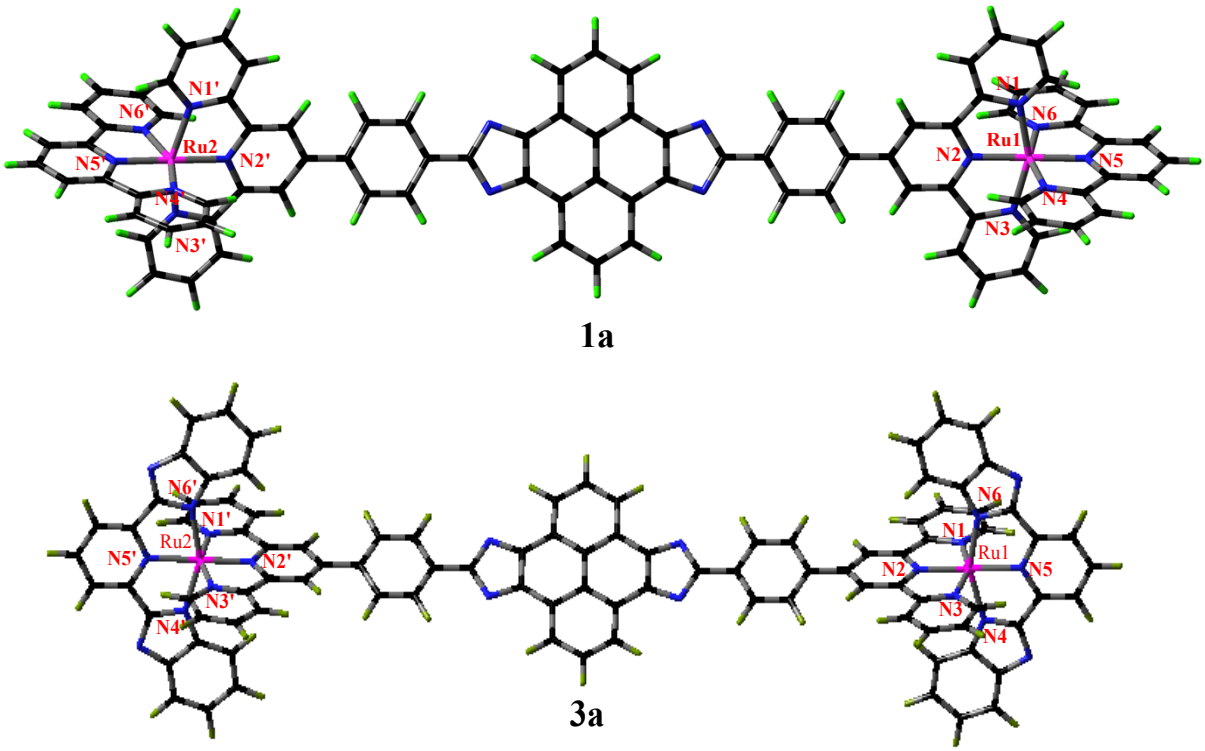

Fig. S29 UKS Optimized geometries and labeling schemes of [(tpy)Ru(tpy-PhImzPy-tpy)Ru (tpy)]$^{2+}$ (**1a**), and [(pbbzim)Ru (tpy-PhImzPy-tpy)Ru(pbbzim)]$^{2-}$ (**3a**) in DMSO.

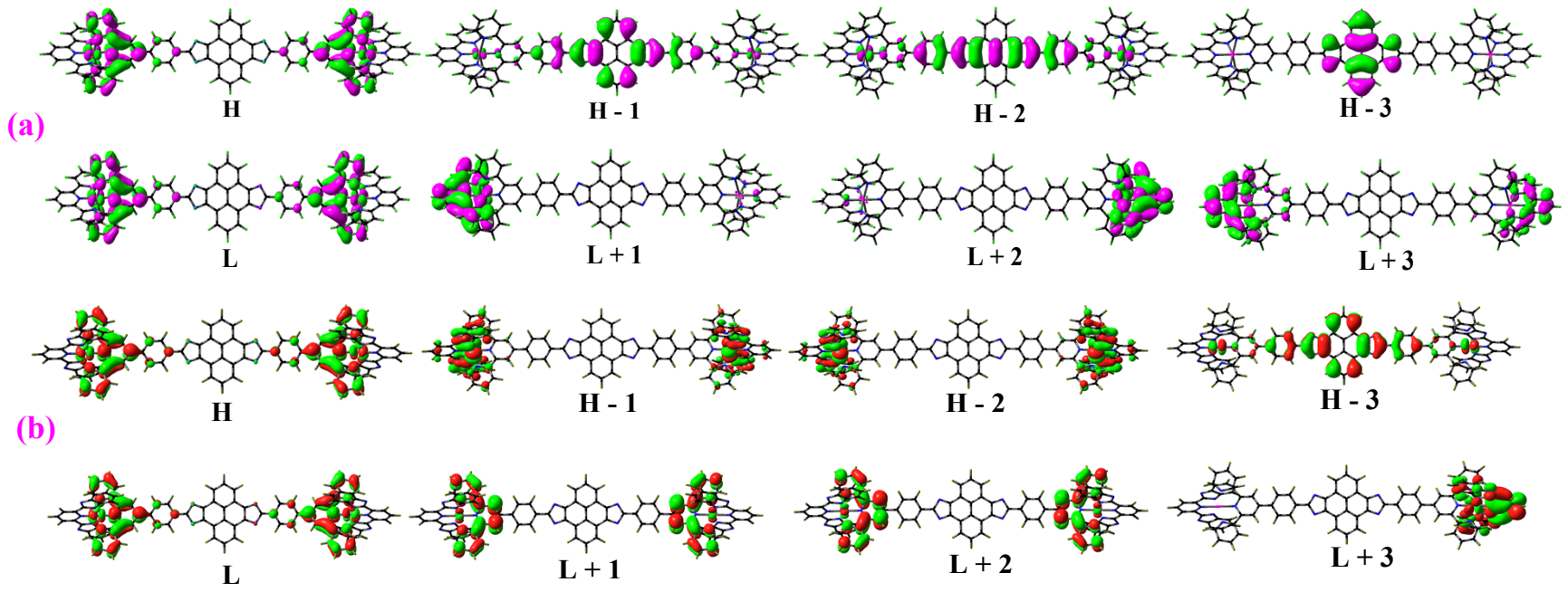

Fig. S30 Schematic drawings of the selective frontier molecular orbitals for **1a** (a)) and **3a** (b) in UKS optimized state in DMSO.

References

S1 M. J. Frisch, G. W. Trucks, H. B. Schlegel, G. E. Scuseria, M. A. Robb, J. R. Cheeseman, G. Scalmani, V. Barone, B. Mennucci, G. A. Petersson, H. Nakatsuji, M. Caricato, X. Li, H. P. Hratchian, A. F. Izmaylov, J. Bloino, G. Zheng, J. L. Sonnenberg, M. Hada, M. Ehara, K. Toyota, R. Fukuda, J. Hasegawa, M. Ishida, T. Nakajima, Y. Honda, O. Kitao, H. Nakai, T. Vreven, J. A. Jr. Montgomery, J. E. Peralta, F. Ogliaro, M. Bearpark, J. J. Heyd, E. Brothers, K. N. Kudin, V. N. Staroverov, R. Kobayashi, J. Normand, K. Raghavachari, A. Rendell, J. C. Burant, S. S. Iyengar, J. Tomasi, M. Cossi, N. Rega, J. M. Millam, M. Klene, J. E. Knox, J. B. Cross, V. Bakken, C. Adamo, J. Jaramillo, R. Gomperts, R. E. Stratmann, O. Yazyev, A. J. Austin, R. Cammi, C. Pomelli, J. W. Ochterski, R. L. Martin, K. Morokuma, V. G. Zakrzewski, G. A. Voth, P. Salvador, J. J. Dannenberg, S. Dapprich, A. D. Daniels, Ö. Farkas, J. B. Foresman, J. V. Ortiz, J. Cioslowski and D. J. Fox, Gaussian 09, revision A.02; Gaussian Inc.: Wallingford, CT, 2009

S2 Becke, A. D *J. Chem. Phys.* **1993**, *98,* 5648-5652.

S3 C. T. Lee, W. T. Yang and R. G. Parr, *Phys. Rev. B* 1988, **37,** 785-789.

S4 P. J. Hay and W. R. Wadt, *J. Chem. Phys.* 1985, **82**, 299-310.

S5 M. E. Casida, C. Jamorski, K. C. Casida and D. R. Salahub, *J. Chem. Phys.* 1998, **108**, 4439-4449.

S6 R. E. Stratmann, G. E. Scuseria and M. J. Frisch, *J. Chem. Phys.* 1998, **109**, 8218-8224.

S7 V. A. Walters, C. M. Hadad, Y. Thiel, S. D. Colson, K. B. Wiberg, P. M. Johnson and J. B. Foresman, *J. Am. Chem. Soc.* 1991, **113**, 4782-4791.

S8 (a) J. Tomasi, B. Mennucci, R. Cammi, *Chem. Rev.* 2005, **105**, 2999-3094; (b) M. Cossi, G. Scalmani, N. Rega, V. Barone, *J. Chem. Phys.* 2002, **117**, 43-54.

S9 R. II. Dennington, T. Keith; J. Millam, *Gauss View 3*; Semichem, Inc.: Shawnee Mission, KS, 2007**.**

S10 N. M.O Boyle, A. L.Tenderholt, K. M. Langner, *J. Comput. Chem*. 2008, **29**, 839-845.